Journal of King Saud University – Engineering Sciences 34 (2022) 23–30

Contents lists available at ScienceDirect

Journal of King Saud University – Engineering Sciences

journal homepage: www.sciencedirect.com

Optimal Design of Ammonia Synthesis Reactor for a Process Industry

Md. Burhan Kabir Suhan [a], Md. Naimur Rahman Hemal [b], M.A.A. Shoukat Choudhury [a,*], Md. Ali Akkas Mazumder [c], Mohaiminul Islam [d]

[a] Department of Chemical Engineering, Bangladesh University of Engineering and Technology (BUET), Dhaka 1000, Bangladesh
[b] Department of Computer Science & Engineering, Military Institute of Science & Technology (MIST), Dhaka 1216, Bangladesh
[c] Karnaphuli Fertilizer Company Limited (KAFCO), Chattogram 4000, Bangladesh
[d] Department of Chemical Engineering, Bangladesh University of Engineering and Technology (BUET), Dhaka 1000, Bangladesh

ARTICLE INFO

Article history:
Received 22 June 2020
Accepted 20 August 2020
Available online 29 August 2020

Keywords:
Modeling
Catalytic bed length
Pressure vessel
Support
Pressure drop

ABSTRACT

Ammonia synthesis is a crucial section of ammonia and urea plant. Many industries are facing a challenge of efficient ammonia production every day. In this study, steady state one dimensional pseudo-homogeneous models of an axial flow industrial catalytic packed bed ammonia converter have been developed. The converter is a vertical two catalytic bed reactor with varying volumes of catalysts. Required industrial data for the design were collected from a fertilizer industry in Bangladesh - and the Halder Topsoe process was followed. Differential equations of the - mathematical model were solved using Runge-Kutta-Fehlberg (RKF45) method by Polymath solver software. For a 23.8% single-pass conversion and for a 3 m inside diameter vessel, a total of 22.5 (15 + 7.5) m catalyst bed was required. Pressure vessel wall and head thickness were found 112 mm and 62 mm respectively. Skirt support was selected and the thickness was calculated 12 mm. Pressure drop along the length of the bed was found 2.55 atm. Finally, parameters of the optimized model were compared with the real industrial data and found quite satisfactory.
© 2020 The Authors. Production and hosting by Elsevier B.V. on behalf of King Saud University. All rights reserved.

1. Introduction

Optimal production of ammonia is vital for developing countries like Bangladesh where the economy mostly depends on agriculture. Several nitrogen compounds such as urea, nitric acid, fertilizer, explosive materials, pharmaceuticals, polymers and coolants can be produced from ammonia. The ammonia synthesis section is considered the heart of the fertilizer plant where ammonia synthesis reactor is a major component of this section. Thus, optimum urea production mostly depends on the efficient way of ammonia production. It is produced following the Haber-Bosch process by the reaction between gaseous nitrogen (collected from air) and hydrogen (from natural gas) (Panahandeh et al., 2003; Gunorubon and Raphael, 2014). A conventional ammonia production process consists of production of the synthesis gas, compression of the gas to the required pressure and synthesis loop of ammonia conversion in a reactor (Baddour et al., 1965).

Multi bed radial flow converter design was introduced at first by Topsoe as technology licensor which improved conversion per pass compared to other known technology. The Topsoe S-200 ammonia synthesis converter is a two-bed radial flow converter with indirect cooling between the catalyst beds. Since the introduction of the S-200 converter type in 1976, it has been used in more ammonia plants than any other converter design, with more than 130 converters installed worldwide (Halder Topsoe).

As per available literature, several designs of industrial reactor by modeling, simulation and performance evaluation were studied in fluidized bed reactor (Fakeeha et al., 1992; Abashar, 2015), membrane reactor (Mirzaee and Mirzaee, 2012; Abashar and Al-Rabiah, 2005), bioreactor (Suhan et al., 2019) and fixed bed reactor (Anisuzzaman et al., 2016; Ali et al., 2017; Abashar, 2018), etc. To the best of our knowledge there is no study has been performed which completely optimized and designed a model of the catalytic reactor including both the internals and externals calculation.

* Corresponding author.
E-mail addresses: suhankabir20@gmail.com (Md. Burhan Kabir Suhan), hemalnaimur@yahoo.com (Md. Naimur Rahman Hemal), shoukat@che.buet.ac.bd (M.A.A. Shoukat Choudhury), akkas.mazumder@kafcobd.com (Md. Ali Akkas Mazumder), buetmohaimin@gmail.com (M. Islam).
Peer review under responsibility of King Saud University.

Production and hosting by Elsevier

https://doi.org/10.1016/j.jksues.2020.08.004
1018-3639/© 2020 The Authors. Production and hosting by Elsevier B.V. on behalf of King Saud University. All rights reserved.

Therefore, this study mainly focused on the reactor part of the ammonia synthesis loop. Optimized length of bed, pressure vessel internals, support and pressure drop along the bed length were calculated based on the data from a real fertilizer industry. Finally, the optimized model parameters were compared with the real industry data.

2. Steps to design

- **Length of bed calculation**: From a known material balance data, required number of catalyst bed and length of each bed were optimized. Besides, an inter-bed heat exchanger was required.
- **Pressure vessel design:** Parameters include- safety factor, maximum safe operating temperature and pressure, material of construction, corrosion allowance, minimum design temperature (for brittle fracture) were taken into consideration before the design of a pressure vessel. Suitable material selection is necessary to handle the extreme situations safely.
  - o **Selection of materials**
  - o **Vessel wall thickness calculations**
  - o **Vessel head thickness calculations**
- **Support:** Cylindrical and other types of vessels need to be supported to withstand its dead weight, the extreme conditions of bending moment created by wind and seismic load. Vertical vessels are generally supported by skirt, bracket and column. The choice for an appropriate type of support depends on height, diameter, available floor space and convenience of location (Mungla, 2016). Tall vessels are usually supported by skirt. Cylindrical skirt is extensively used to support cylindrical vessels (Joshi, 1976).
  - o **Selection of support**
  - o **Thickness calculation**
- **Pressure drop along the length of bed:** Pressure drop of fluid when penetrating the bed is considered one of the most important parameters in design. Ergun first proposed the correlations for pressure drop calculation Ergun, 1952. However, large number of correlations were established based on Ergun correlations in the literature. In this study, Ergun correlation was used.

3. Mathematical model development

By modeling synthesis reactor- temperature, conversions, reaction rate and equilibrium constant profiles are obtained. Testing of the model based on the above parameters is achieved at the end of each bed as industrial data are not usually available along the length of the bed. The following assumptions have been made for this modeling (Dashti et al., 2006)-

1. One-dimensional coordinate has been considered along with the bulk flow.
2. The penetration of mass and heat is ignored, as the fluid velocity is very high on the industrial scale.
3. Pressure and density are constant.
4. Concentration and temperature on catalyst surface and bulk of gas are equal.
5. The thermal and concentration gradients in the radial direction are negligible.
6. The effects of penetration resistance in catalyst, temperature gradient and catalyst inside concentration have been incorporated in the equations by a coefficient.

3.1. Material balance (Molar)

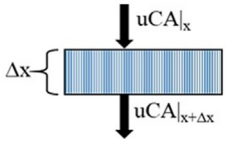

Considering an element with height of Δx and cross section area (A) equal to that of the bed we'll have (Elnashaie et al., 1988; Dashti et al., 2006)

Accumulation = Consumption – Production + Output – Input

There shall be no accumulation as the system has been considered to be in a steady state. Considering uCA the molar flowrate, Eqn. (1) can be obtained.

$$uCA|_x - uCA|_{x+\Delta x} - A\Delta x(R_{NH3})\eta = 0 \quad (1)$$

Dividing both sides of the Eqn. (1) by $A\Delta x$ and $\Delta x \to 0$, we get Eqn. (2).

$$-u\frac{dc}{dx} - \eta R_{NH3} = 0 \quad (2)$$

Eqn. (2) can be re-written as Eqn. (3) based on the nitrogen conversion shown by X_{N2} and length of the bed by L.

$$\frac{dX_{N2}}{dL} = \frac{\eta R_{NH3} A}{2F_{N2}} \quad (3)$$

Where, X_{N2} = reactant conversion, L = length of the reactior, η = effectiveness factor of the catalyst, R_{NH3} = rate of reaction.

3.2. Energy balance

Energy balance for the differential element in the catalyst bed of converter yields-

Accumulation = Consumed Energy – Produced Energy + Output Energy – Input Energy

In steady state, the accumulation is zero.

$$A\left(F_{total}C_{pmix}T|_x - F_{total}C_{pmix}T_{|x+\Delta x}\right) = \eta(-\Delta H_R)A\Delta x R_{NH3} \quad (4)$$

Dividing both sides of the Eqn. (4) by $A\Delta x$, $\Delta x \to 0$ and length of bed denoted by L we get Eqn. (5).

$$\frac{dT}{dL} = \frac{\eta\,(-\Delta H_R)A\,R_{NH3}}{F_{total}C_{pmix}} \quad (5)$$

Where, $-\Delta H_R$ = heat of reaction (kj/kmol), F_{total} = total molar flow rate (kmole), C_{pmix} = specific heat of the reacting mixture, A = area of the reactor

3.3. Heat of reaction and specific heat capacity of the mixture

Mahfouz et al. developed a suitable expression for calculating exothermic heat of reaction (Mahfouz et al., 1987; Gunorubon and Raphael, 2014). As the ammonia production (forward reaction) is an exothermic process, this expression has been used in this study.

$$\Delta H_R = 4.184\left\{-\left[0.54526 + \frac{840.609}{T} + 459.734 \times \frac{10^6}{T^3}\right]p - 5.34685T - 0.2525 \times 10^{-3}T^2 + 1.69167 \times 10^{-6}T^3 - 9157.09\right\}\left(\frac{kj}{kmol}\right) \quad (6)$$

Following the individual component specific heat expression from Shah study, Elverse et al. determined the expression for the heat capacities of the components of the reactant gases and product ammonia gas mixture using the Eqn. (7) expression and is presented in Eqn. (8) (Shah, 1967; Elverse et al., 1993). From the expression molar specific heat of the mixture was found to vary with the temperature (T) and pressure (P) where P is in kPa unit and T is in kelvin unit.

$$C_p = \sum y_i C_{pi} \tag{7}$$

$$C_{pmix} = 35.31 + .02T + .00000694\,T^2 - .0056\,P + .000014PT \quad \left(\frac{KJ}{Kmol}\right) \tag{8}$$

where, y_i = mole fraction of component i, C_{pi} = specific heat capacity of component i.

3.4. Chemistry and kinetics

The overall stoichiometric equation is

$$N_2 + 3H_2 \rightarrow 2NH_3 \tag{9}$$

Extensive studies of ammonia synthesis on iron catalysts suggests that the reaction occurs through surface imine radicals and the following elementary steps (Nielsen, 1971)

$$N_2(g) \rightarrow 2\ N(ads) \tag{10}$$

$$H_2(g) \rightarrow 2H(ads) \tag{11}$$

$$N(ads) + H(ads) \rightarrow NH(ads) \tag{12}$$

$$NH(ads) + H(ads) \rightarrow NH_2(ads) \tag{13}$$

$$NH_2(ads) + H(ads) \rightarrow NH_3(ads) \tag{14}$$

$$NH_3(ads) \rightarrow NH_3(g) \tag{15}$$

A rate equation based on nitrogen adsorption as the slow step. The reaction rate expression is represented as:

$$R_{NH3} = 2k\left(k_a^2 a_{N2}\left[\frac{(a_{H2})^3}{(a_{NH3})^2}\right]^{\alpha} - \left[\frac{(a_{NH3})^2}{(a_{H2})^3}\right]^{1-\alpha}\right)\frac{kmol}{m^3 - hr} \tag{16}$$

where, α = constant which takes a value form 0.5 to 0.75 in literature (Nielsen, 1971; Dashti et al., 2006), k = rate constant for the reaction, k_a = equilibrium constant, a_i = activity of i component

The reaction rate equations for the reactants were determined using the stoichiometry of the reaction and value of α was selected 0.5. Individual reaction rates are related as such :

$$-R_{N2} = -\frac{1}{3}R_{H2} = \frac{1}{2}R_{NH3} \tag{17}$$

Activation can be written in terms of the activation coefficient as below (Dashti et al., 2006)

$$a_i = \frac{f_i}{f_i^0} \tag{18}$$

f_i^0 : Reference fugacity. If the reference fugacity is considered to be 1 atm, then:

$$a_i = \frac{f_i}{1} = f_i = y_i\phi_i P \tag{19}$$

Here, y_i denotes the mole fraction of individual component in gas mixture of reversible reaction, ϕ_i denotes the fugacity coefficients and P denotes the pressure of gas mixture.

The fugacity coefficients for nitrogen (N_2), hydrogen (H_2) and ammonia (NH_3) were determined using the following expressions (Eqn. (20)–(22)) where T is in kelvin unit and P is in atmosphere unit (Dyson and Simon, 1968; Dashti et al., 2006).

$$\Phi_{N2} = 0.93431737 + 0.2028538\times10^{-3}T + 0.29589610^{-3}P - 0.270727\,10^{-6}T^2 + 0.4775207\times10^{-6}P^2 \tag{20}$$

$$\Phi_{H2} = exp\left\{exp\left(-3.8402\ T^{0.125} + 0.541\right)\times P - exp\left(-0.1263\ T^{0.5} - 15.98\right)\times P^2 + 300\times exp(-0.011901\ T - 5.941)\times exp(-P/300)\right\} \tag{21}$$

$$\Phi_{NH3} = 0.1438996 + 0.2028538\times10^{-2}T - 0.4487672\times10^{-3}P - 0.1142945\times10^{-5}T^2 + 0.2761216\times10^{-6}P^2 \tag{22}$$

The mole fraction of each component (y_i) were expressed in terms of fractional conversion of the limiting reactant nitrogen (X) developed by performing a mole balance on the converter where Y_i denotes the initial mole fraction of each component before reaction proceed.

$$y_{N_2} = \frac{Y_{N_2}(1-X)}{1-2XY_{N_2}} \tag{23}$$

$$y_{H_2} = \frac{Y_{H2} - 3XY_{N2}}{1-2XY_{N2}} \tag{24}$$

$$y_{NH_3} = \frac{Y_{NH3} + 2XY_{N2}}{1-2XY_{N2}} \tag{25}$$

Using Eqn. (23)–(25) component activities in Eqn. (19) can be expressed and further substituted in Eqn. (15) to yield the reaction rate expression in terms of fractional conversion of the limiting reactant nitrogen (Eqn. (26)) (Rase and Homes, 1977).

$$R_{NH_3} = 2k\left[\frac{k_a^2\ \phi_{N2}\ Y_{N_2}(1-X)P}{1-2XY_{N_2}}\times\left\{\frac{p(\phi_{H2}(Y_{H2}-3XY_{N2}))^3}{(1-2XY_{N2})(\phi_{NH3}(Y_{NH3}+2XY_{N2}))^2}\right\}^{\alpha} - \left\{\frac{(1-2XY_{N2})\phi_{NH3}(Y_{Nh3}+2XY_{N2})}{P(\phi_{H2}(Y_{H2}-3XY_{N2}))^3}\right\}^{1-\alpha}\right]\frac{kmol}{m^3-hr} \tag{26}$$

The rate constant for the reversible reaction was obtained using the arrhenius relation with values for the synthesis reaction given by (Dashti et al., 2006)

$$k = k_o e^{-\frac{E}{RT}} \tag{27}$$

Where, K_0 = arrhenius coefficient = 8.849×10^{14}, E = activation energy with temperature = mean value 170560 kJ/kmol, R = universal gas constant (8.314 kJ/kmol.K)

3.5. Equilibrium constant

The formation of ammonia is a reversible and exothermic reaction which can proceed both in forward direction (ammonia synthesis) and backward direction (ammonia decomposition). The reaction is accompanied by decrease in volume because there is a decrease in number of moles of gas. By Le Chatelier's Principle, increasing the pressure and decreasing the temperature causes the equilibrium to shift to the right resulting in a higher yield of ammonia since there is a pressure drop accompanying the transformation and also releases heat. is an equilibrium reaction that is favoured by low temperature and high pressure (Modak, 2002). Gillespie and Beattie developed the Eqn. (28) to calculate the equilibrium constant in 1930 which is applicable for wide

range of temperatures and pressures in ammonia synthesis reaction (Gillespie and Beattie, 1930).

$$\log_{10}k_a = -2.691122\log T - 5.519265 \times 10^{-5}T + 1.848863 \times 10^{-6}T^2 + \frac{2001.6}{T} + 2.689 \quad (28)$$

3.6. Effectiveness factor

The relation between the rate of formation of ammonia and the temperature, pressure, composition in the bulk gas phase can be obtained with Eqn. (26) for fine catalyst (no diffusion restriction) will be used as the sufficiently fine particle size exclude the possibility of interaction of kinetic and transport effects. However, catalyst particles of 6–10 mm size are subject to diffusion restriction in their pore structure. Thus the rate equation is to be multiplied by effectiveness factor and some modifications to be imposed as well as some modifications to include the effects of particle size on reduction, poisoning, density of the catalyst interior and catalyst aging. Effectiveness factor is defined as the rate at which the reaction occurs in a pellet divided by the rate at which the reaction would occur if the concentration and temperature throughout the pellet were the same as those at the surface. To evaluate the effectiveness factor Dyson and Simon proposed Eqn. (29) where the constants were evaluated at 150 atm, 225 atm and 300 atm. In order to avoid the relatively difficult task of solving the nonlinear two-point boundary value differential equation along the length of the reactor, this empirical relation is quite useful and was suggested by several previous study (Dyson and Simon, 1968; Rase and Homes, 1977; Dashti et al., 2006; Anne and Goli, 2012).

As our process operates at 129 atm, constant values were taken from 150 atm chart (nearest pressure among them) of Dyson et al evaluated chart (Dyson and Simon, 1968).

$$\eta = b_0 + b_1T + b_2X + b_3T^2 + b_4X^2 + b_5T^3 + b_6X^3 \quad (29)$$

Constants are

$b_0 = -17.539096$, $b_1 = .07697849$, $b_2 = 6.900548$, $b_3 = -1.082 \times 10^{-4}$, $b_4 = -26.4247$, $b_5 = 4.9276 \times 10^{-8}$, $b_6 = 38.937$

4. Results and discussion

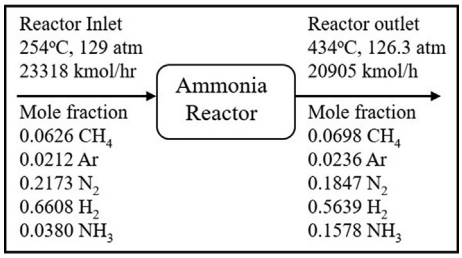

The modelling design was performed based on the block diagram data collected from the fertilizer industry located in Bangladesh. The single-pass conversion of N_2 along the ammonia converter was selected 23.8% (Halder Topsoe).

4.1. Length of bed calculation

The objective of Polymath Solver software is to provide a solution for a system of simultaneous first-order ordinary differential equations and explicit algebraic equations. This software is mostly suitable for chemical engineering problem-solving. Thus in the current study, ordinary differential equations of Eqn. (3) and Eqn. (5) were solved simultaneously using the software and following results were achieved.

From the conversion profile of 1st converter bed in Fig. 1, it can be seen that after 15 m length the conversion significantly decreased. The same result was obtained from the reaction rate profile where the rate reduced after 15 m. So a converter bed of 15 m will be suitable for the first bed. The conversion percentage after 1st converter is found 19% and the temperature at the inlet of 1st bed is 360 °C (633 °K) and the outlet temperature is found 442 °C (715 °K). 1st converter bed outlet is passed through inter bed heat exchanger and the temperature reduced to 377 °C (650°K).

From the conversion profile of 2nd converter bed in Fig. 2, it can be seen that after 7.5 m length the conversion significantly decreased and at this point, the conversion reached our desired 23.8%. From the reaction rate profile, it can also be seen that the rate is about to reduce after 7.5 m. So a converter bed of 7.5 m will be suitable for the second bed. The temperature at the inlet of the 2nd bed is 377 °C (650 K) and the outlet temperature is found 397 °C (670 °K).

Fig. 3 is illustrated for observing the relation of conversion and ammonia equilibrium with respect to temperature. From Fig. 4, it can be observed that when the length of the 1st bed approaching 15 m the conversion percentage tends to decrease due to the exothermic reaction increasing the temperature of the reacting mixture. Therefore, an inter bed heat exchanger should be used to get a better conversion percentage in a minimum length of bed by cooling the reacting mixture. The mixture was passed to the second catalyst bed followed by cooling duty. Increasing trend can be seen on effectiveness factor profile due to the rise of temperature and conversion along the length of catalyst bed Fig. 4.

So, the length of the 1st ammonia converter bed is 15 m, 2nd ammonia converter bed is 7.5 m and the total length of the bed is 22.5 m.

4.2. Pressure vessel design

Related data for pressure vessel design are as follows-

Design pressure = 155 $\frac{kg}{cm^2.g}$, working pressure = 140 $\frac{kg}{cm^2.g}$, design temperature = 370 °C, corrosion allowance (head/shell) = 1.6 mm, insulation thickness = 100 mm, inside diameter = 3000 mm, outside diameter = 3224 mm, safety factor = 1.5

4.2.1. Material Selection

ASME SA542 Grade B Class 4

SA542 has five grades or levels. They are- grade A, grade B, grade C, grade D, grade E. SA542 Grade B Class 4 need to be done heat-treatment to meet the property requirement in the standard ASTM SA-542. SA542 Grade B Class 4 in the standard SA-542 is a kind of Mo-V alloy steel plate material used to fabric high-temperature pressure vessels. Hence, it has been selected and the compositions (heat analyse) are as follows (Shanghai Royal; HZZ Iron and Steel)

C 0.09 ~ 0.18, Mn 0.25 ~ 0.66, P ≤ 0.015, S ≤ 0.015, Si ≤ 0.50, Ni ≤ 0.28, Cr 1.88 ~ 2.62, Mo 0.85 ~ 1.15, V ≤ 0.03, Cu ≤ 0.28

4.2.2. Vessel wall thickness calculation

The ratio of outside diameter to inside diameter = $\frac{3224}{3000}$ = 1.075 < 1.5

Thus, the design procedure is followed by M.V. Joshi's Process Equipment Design book (Joshi, 1976).

$$\text{Circumferential stress; } f_D = \frac{pD}{2t} \quad (30)$$

$$\text{Longitudinal or axial stress } f_a = \frac{pD}{4t} \quad (31)$$

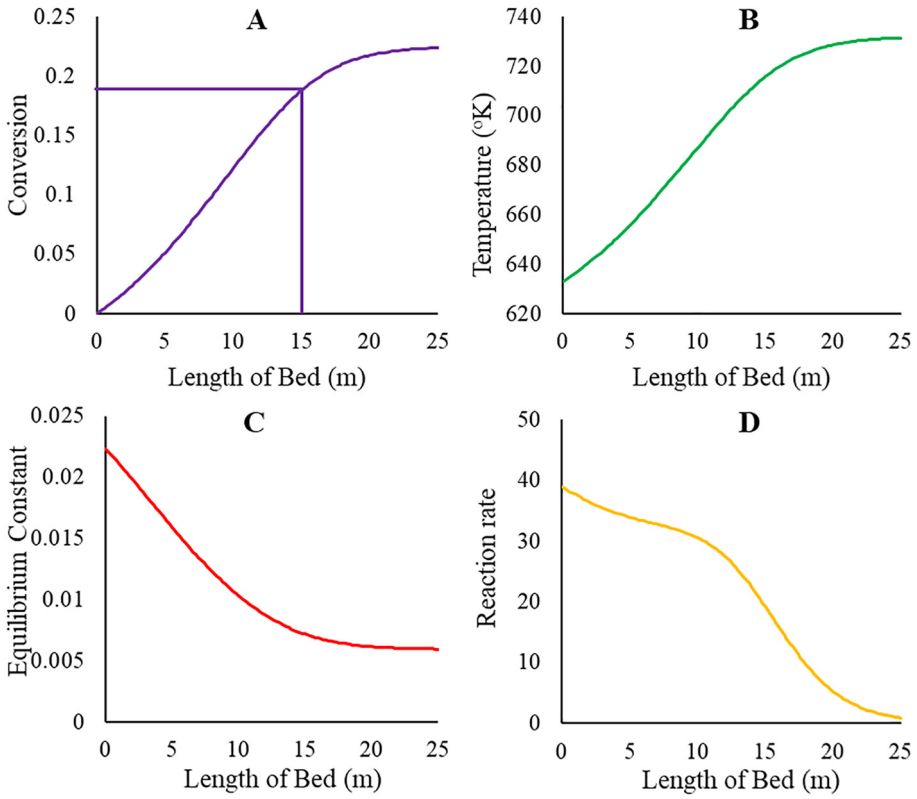

Fig. 1. A) Conversion B) Temperature C) Equilibrium constant and D) Reaction rate profile for the 1st converter bed.

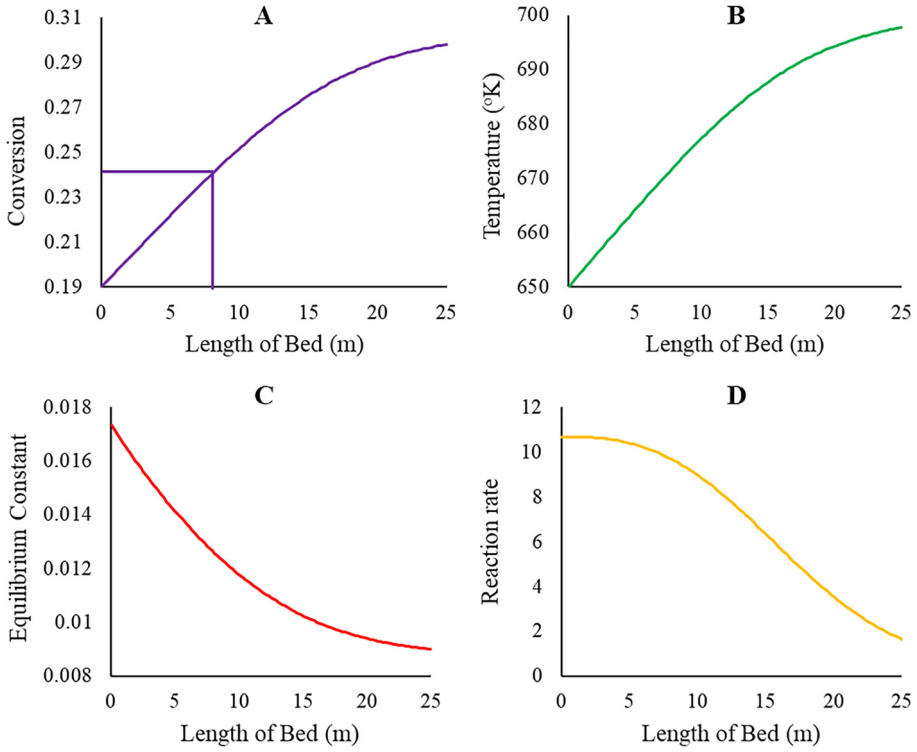

Fig. 2. A) Conversion B) Temperature C) Equilibrium constant and D) Reaction rate profile for the 2nd converter bed.

Where, p = internal pressure, D = mean diameter of the shell

Circumferential stress is greater than the longitudinal stress. So, circumferential stress is selected as design stress. The shell is generally formed by a joint in the longitudinal direction, which is considered in terms of joint efficiency. The shell thickness is therefore,

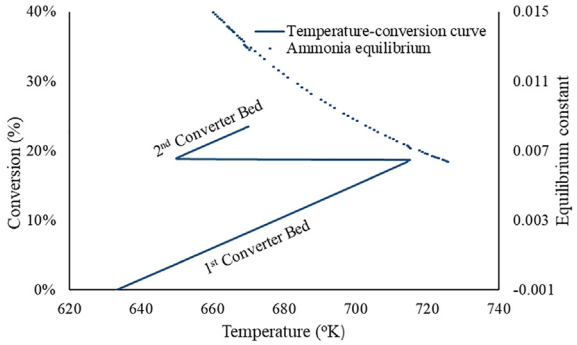

Fig. 3. Conversion and equilibrium constant vs temperature.

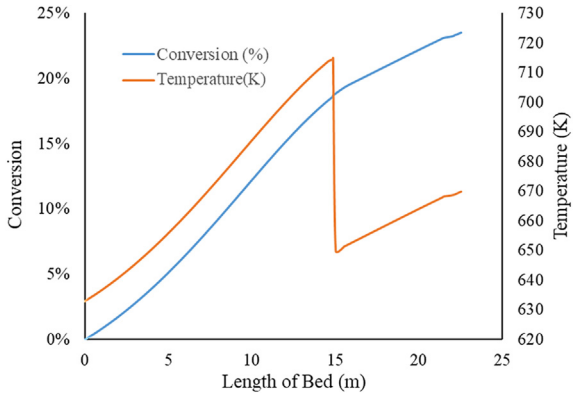

Fig. 4. Conversion, temperature and effectiveness factor profile along the length of bed.

$$t = \frac{pD_i}{2\frac{f}{s}j - p} \tag{32}$$

p = design pressure = 155 $\frac{kg}{cm^2}$, j = joint efficiency = 1, D_i = internal diameter = 3000 mm , T = design temperature = 370 °C, f = design or permissible stress at 370 °C = 322.8 MPa = 3291.64 $\frac{kg}{cm^2}$, S = safety factor = 1.5

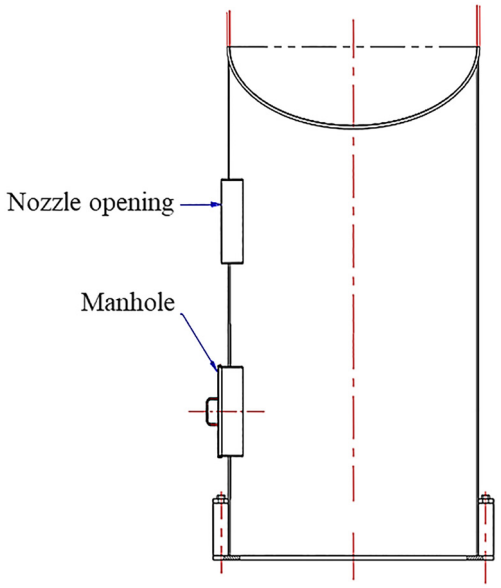

Fig. 5. Cylindrical skirt support (Mungla, 2016).

Shell thickness, t = $\frac{155\frac{kg}{cm^2} \times 3000 \text{ mm}}{2\times\frac{3291.64}{1.5}\frac{kg}{cm^2}\times 1 - 155\frac{kg}{cm^2}}$ =109.83 mm

Corrosion allowance of 1.6 mm will be used.

Final wall thickness = (109.83 + 1.6) mm = 111.43 mm ≈ 112 mm

4.2.3. Vessel head thickness calculation

Ellipsoidal head, hemispherical head and torispherical head are three types of ASME pressure vessel dished heads. A sphere is the ideal shape for a head, because the pressure in the vessel is divided equally across the surface of the head. The radius (R) of the head equals the radius of the cylindrical part of the vessel. Thus, hemispherical head is selected for the design.

Inside diameter = 3000 mm, Outside diameter, D_o = 3150 mm, s = safety factor = 1.5, B = 1.1

$$\text{Head thickness; } t = \frac{pD_oB}{4\frac{f}{s}j + p} \tag{33}$$

$$= \frac{155\frac{kg}{cm^2} \times 3150 \text{ mm} \times 1.1}{4 \times \frac{3291.64}{1.5}\frac{kg}{cm^2} \times 1 + 155\frac{kg}{cm^2}} = 60.12 \text{ mm}$$

Corrosion allowance of 1.6 mm will be used.

Final head thickness = (60.12 + 1.6) mm = 61.72 mm ≈ 62 mm

4.3. Support Selection and calculation

The pressure vessel is supported on cylinder, welded directly to the bottom head. The skirt consists of various cut outs for outlet nozzles & manholes (Fig. 5). The skirt not only allows the vessel to be placed at required height in the plant but also allow proper bolting arrangement with civil foundation. The thickness of the skirts is calculated using combined force theory (Joshi, 1976; Mungla, 2016). The cylindrical shell of the skirt is designed for the combination of stresses due to vessel dead weight, wind load and seismic load. The skirt thickness is uniform and is design to withstand maximum tensile and compressive stresses (Joshi, 1976).

4.3.1. Stress due to dead weight for skirt support

$$f_d = \frac{\sum W}{\pi D_{ok} t_{ok}} \tag{34}$$

f_d = stress due to dead weight, W = dead weight of catalyst filled vessel contents and attachments = 401,500 kg, D_{ok} = diameter of the skirt = 3.224 m, t_{ok} = thickness of the skirt.

$$f_d = \frac{\sum W}{\pi D_{ok} t_{ok}} = \frac{401,500}{\pi \times 3.224 \times t_{ok}} = \frac{39640}{t_{ok}} \frac{kg}{m^2}$$

4.3.2. Stress due to bending moment created by wind

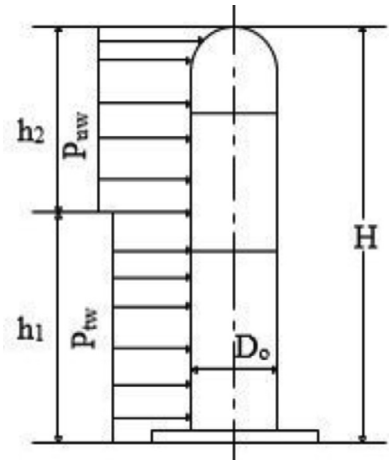

$$f_{wb} = \frac{M_w}{Z} = \frac{4M_W}{\pi D_0^2 t_{sk}} \tag{35}$$

Z = Modulus of section for skirt cross-section
t_{sk} = thickness of the skirt
For total height greater than 20 m,

$$M_w = p_{tw}\frac{h_1}{2} + p_{uw}\left(h_1 + \frac{h_2}{2}\right) \tag{36}$$

$$p_{tw} = k\ p_1\ h_1\ D_o \tag{37}$$

$$p_{uw} = k\ p_2\ h_2\ D_o \tag{38}$$

P_1 = wind pressure for the lower part of the vessel (40 to 100 $\frac{kg}{m^2}$) = 100 $\frac{kg}{m^2}$
P_2 = wind pressure for the upper part of the vessel (upto 200 $\frac{kg}{m^2}$) = 200 $\frac{kg}{m^2}$
D_o = Outside diameter of the vessel = 3.224 m
k = Coefficient depending on the shape factor = 0.7 (for cylindrical surface)

$$f_{wb} = \frac{4M_W}{\pi D_0^2 t_{sk}} = \frac{p_{tw}\frac{h_1}{2} + p_{uw}\left(h_1 + \frac{h_2}{2}\right)}{\pi D_0^2 t_{sk}} = \frac{kp_1\ h_1\ D_o\left(\frac{h_1}{2}\right) + k\,p_2\ h_2\ D_o\left(h_1 + \frac{h_2}{2}\right)}{\pi D_0^2 t_{sk}} \tag{39}$$

h_1 = 20 m
h_2 = 22.5 (Total length of bed) – 20 (upper limit of h_1) + 1.5 (Head radius) + 5 (Height of the skirt)
= 9 m

$$f_{wb} = 4 \times \frac{0.7 \times 100 \times 20 \times \left(\frac{20}{2}\right) \times 3.224}{\pi \times (3.224)^2 \times t_{sk}} + \frac{0.7 \times 200 \times 9 \times 3.224 \times \left(20 + \frac{9}{2}\right)}{\pi \times (3.224)^2 \times t_{sk}} = \frac{4}{32.65} \times \frac{144660}{t_{sk}}\frac{kg}{m^2} = \frac{17722.51}{t_{sk}}\frac{kg}{m^2}$$

4.3.3. Stress due to seismic load

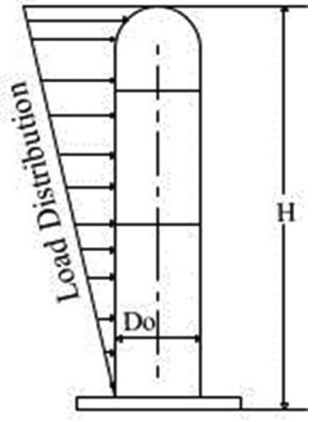

$$f_{sb} = \frac{8CWH}{3\pi D_0^2 t_{sk}} \tag{40}$$

C = Seismic coefficient = 0.1 (Typically 0.1 to 0.3)
W = Total weight of vessel
H = Height of vessel

$$f_{sb} = \frac{8 \times 0.2 \times 401500 \times 29}{3\pi \times 3.224^2 \times t_{sk}} = \frac{95084}{t_{sk}}\frac{kg}{m^2}$$

4.3.4. Thickness calculation

Possibility of the wind load and earthquake load operating simultaneously is very low. Thus, both of them are calculated separately and most adverse loading condition is used to calculate the maximum resultant stress.

Maximum tensile strength at bottom,

$$f_t = \frac{95084}{t_{sk}}\frac{kg}{m^2} - \frac{39640}{t_{sk}}\frac{kg}{m^2} = \frac{55444}{t_{sk}}\frac{kg}{m^2}$$

Maximum allowable tensile strength and yield strength for the material is 73,929,425 $\frac{kg}{m^2}$ and 59,653,300 $\frac{kg}{m^2}$ (Shanghai Royal).
So, $t_{sk} = \frac{55444}{73929425} \approx 0.75$ mm [For tensile strength]
Maximum compressive strength,

$$f_c = \frac{95084}{t_{sk}}\frac{kg}{m^2} + \frac{39640}{t_{sk}}\frac{kg}{m^2} = \frac{134724}{t_{sk}}\frac{kg}{m^2}$$

f_c permissible $\leq \frac{\text{yield stress}}{\text{safety factor}}$
$\leq 59653300/4 = 14913325\ \frac{kg}{m^2}$
So, t_{sk} = 134724/14913325 m ≈ 9 mm [For compressive stress]
We will use a thickness of 12 mm for the skirt.

4.4. Pressure drop calculation

The pressure drop through a gas–solid packed bed can be described by the equation first proposed by Ergun (1952) and supported by other studies (Zhao et al., 2000).

$$\frac{\Delta P}{L} = \text{viscous energy loss} + \text{kinetic energy loss} = \frac{150\mu(1-\varepsilon)^2}{D_p^2 \times \varepsilon^3} v_s + 1.5\,\frac{v_s^2 \rho (1-\varepsilon)}{D_p \varepsilon^3} \tag{41}$$

Height, L = 22.5 m

$$\text{Volumetric GasFlowrate} = \frac{\text{Molar flowrate} \times Mw}{\rho} = \frac{23317 \times 9.437}{0.494} = 445430.73 m^3/h$$

$$\text{Superficial Gas Velocity} = \frac{\text{Volumetric flowrate}}{\text{flow area}} = \frac{445430.73}{\pi \times 3^2 \times 3600} = 4.376 m/s$$

Viscosity, $\mu = 2.254 \times 10^{-5}$ Pa.s
Diameter, D_P = 3 mm (Assuming sphericity = 1)
Bed Porosity, ε = 0.6 (Assumed)

Table 1
Comparison of industry data and designed model.

Parameters	Industry data	Design data	Deviation (%)
Outlet H_2 (mole %)	56.4	58.82	4.29
Outlet N_2 (mole %)	18.47	17.45	5.54
Outlet NH_3 (mole %)	15.78	14.9	5.56
1st bed inlet temperature (°K)	633	633	–
1st bed outlet temperature (°K)	755	715	5.29
2nd bed inlet temperature (°K)	650	650	–
2nd bed outlet temperature (°K)	715	670	6.29
Length of catalyst bed (m)	22.7	22.5	0.88
Vessel wall thickness (mm)	112	111.43	0.51
Vessel head thickness (mm)	75	62	17.3
Support thickness (mm)	13	12	7.14
Pressure drop (atm)	2.7	2.55	5.56

Particle Density, ρ = 0.494 kg/m^3
Average molecular weight, Mw = 9.437 kg/kmol

$$\frac{\Delta P}{L} = \frac{150 \times 2.254 \times 10^{-5} \times (1-0.6)^2}{0.003^2 \times 0.6^3} \times 4.376 + 1.75 \frac{4.376^2 \times 0.494 \times (1-0.6)}{0.003 \times 0.6^3} = 11436.63 \frac{Pa}{m}$$

Δp = 257324 Pa = 2.55 atm

4.5. Model validation

The parameters of the designed reactor have been compared with the real industry data in Table 1. Inlet compositions for model were the same as industry during solving equations and the outlet compositions were found to vary a negligible amount. The maximum deviation was found for NH_3 composition, which is nearly 5.56%. In addition, the 1st and 2nd bed inlet temperatures used in the model were the same as industry data and outlet temperatures were observed. Maximum deviation was found in the 2nd bed outlet temperature, which was nearly 6.29%. However, other findings of this study were also compared with industry data. The calculated pressure drop deviated by 5.56% from the industry data. The length of the catalyst bed and the vessel wall thickness were nearly the same as industry. Support thickness was also in acceptable range and only vessel head thickness required was a lower value than that used in the industry. From the comparison in Table 1, it can be said that the designed model matched the industry data quite satisfactorily.

5. Conclusion

As the global demand of ammonia increasing rapidly, optimal design of ammonia production process is a major concern for engineers and researchers. In order to design an ammonia synthesis reactor, one dimensional pseudo homogenous model was developed in this study. From the first principles using material and energy balances on the ammonia converter and equations solving via Polymath solver, the conversion and temperature variations within the catalyst bed were predicted. After predicting the length of bed, pressure vessel design, skirt support design and pressure drop along the reactor were also studied. Quite satisfactory model results were obtained in comparison with a real plant data. It can be concluded that, the study will enrich knowledge of all the readers as well as researchers and also help them to design an ammonia synthesis reactor quite easily and efficiently.

Declaration of Competing Interest

The authors declare that they have no known competing financial interests or personal relationships that could have appeared to influence the work reported in this paper.

References

Abashar, M.E.E., Al-Rabiah, A.A., 2005. Novel multi-shell membrane reactor for efficient dehydrogenation of ethylbenzene. J. King Saud Univ. Eng. Sci. 18 (1), 117–137.
Abashar, M.E.E., 2015. Parametric sensitivity analysis to investigate heptane reforming in circulating fast fluidized bed membrane reactors. J. King Saud Univ. Eng. Sci. 27 (1), 1–13.
Abashar, M.E.E., 2018. Ultra-clean hydrogen production by ammonia decomposition. J. King Saud Univ. Eng. Sci. 30 (1), 2–11.
Ali, E., Al-haj Ali, M., Alhumaizi, K., Elharbawi, M., 2017. Optimal oxygen feeding policy to maximize the production of Maleic anhydride in unsteady state fixed bed catalytic reactors. J. King Saud Univ. Eng. Sci. 29 (3), 204–211.
Anisuzzaman, S.M., Bono, A., Krishnaiah, D., Tan, Y.Z., 2016. A study on dynamic simulation of phenol adsorption in activated carbon packed bed column. J. King Saud Univ. Eng. Sci. 28 (1), 47–55.
Anne S. B., Goli, V. R., 2012. Mathematical modelling of Ammonia converter. International conference on chemical, civil and environment engineering (ICCEE'2012), Dubai.
Baddour, R.F., Brian, P.L.T., Logeais, B.A., Eymery, J.P., 1965. Steady-state simulation of an ammonia synthesis converter. Chem. Eng. Sci. 20 (4), 281–292. https://doi.org/10.1016/0009-2509(65)85017-5.
Dashti, A., Marvast, M.A., Kakavand, M., 2006. Modeling and simulation of ammonia synthesis reactor. Petroleum & Coal. 48 (2), 15–23.
Dyson, D.C., Simon, J.M., 1968. Kinetic expression with diffusion correction for ammonia synthesis on industrial catalyst. Ind. Eng. Chem. Fund. 7 (4), 605–610.
Elnashaie, S.S., Abashar, M.E., Al-ubaid, A.S., 1988. Simulation and optimization of an industrial ammonia reactor. Ind. Eng. Chem. Res. 27, 2015–2022.
Elverse, B., Hawkins, S., Russey, G., Schulz, G., 1993. Ullmann's encyclopedia of industrial chemistry-fifth edition. Principles of chemical reaction engineering and plant design. B(4), 85–98.
Ergun, S., 1952. Fluid flow through packed columns. Chem. Eng. Prog. 48 (2), 89–94.
Fakeeha, A.H., Wagialla, K.M., Al-Shriahy, F.A., 1992. Modelling and simulation of acrylonitrile synthesis from propylene using fluidized bed technology. J. King Saud Univ. Eng. Sci. 4 (2), 127–141.
Gillespie, L.J., Beattie, J.A., 1930. The thermodynamic treatment of chemical equilibria in systems composed of real gases. i. an approximate equation for the mass action function applied to the existing data on the haber equilibrium. Phys. Rev. 36 (4), 743–753.
Gunorubon, A.J., Raphael, N.R., 2014. Simulation of an ammonia synthesis converter. Can. J. Pure. Appl. Sci. 8 (2), 2913–2923.
Halder Topsoe. Ammonia converter baskets S-200. [Online]. Available: https://www.topsoe.com/products/equipment/ammonia-converter-baskets-s-200?hsLang=en. [Last accessed: 13-Aug-2020].
HZZ Iron and Steel.[Online]. Available: http://www.hzzsteel.com.cn/news_detail/newsId=1cfcfcad-8d4d-471c-9e5f-5881a92d8489.html. [Last accessed: 10-Aug-2020].
Joshi, M. V., 1976. Pressure vessels. Process equipment design. 113–189.
Mahfouz, A.T., Elshishini, S.S., Elnshaie, S.S.E.H., 1987. Steady State Modeling and Simulation of an Industrial Ammonia Synthesis Reactor. Reactor modeling, simulation & control. ASME Press. 10 (3), 1.
Mirzaee, H., Mirzaee, F., 2012. Modeling and simulation gas separation by membrane of poly dimethyl siloxane. J. King Saud Univ. Eng. Sci. 24 (1), 35–43.
Modak, J.M., 2002. Haber Process for Ammonia Synthesis. Resonance., 69–77
Mungla, M.J., 2016. Design and analysis of pressure vessel skirt considering seismic load as per uniform building code. Int. J. Eng. Res. Technol. 4 (10), 1–5.
Nielsen, A., 1971. Review of ammonia catalysis. Catal. Rev. Sci. Eng. 4 (1), 1–26.
Panahandeh, M.R., Fathikaljahi, J., Taheri, M., 2003. Steady-state modeling and simulation of an axial-radial ammonia synthesis reactor. Chem. Eng. Tech. 26 (6), 666–671.
Rase, H.F., Homes, J.R., 1977. Case studies and design data. Chemical reactor design for process plants. John wiley & sons, inc., pp. 61–85.
Shah, M., 1967. Control simulation in ammonia production. Ind. Eng. Chem. 59 (1), 72–83. https://doi.org/10.1021/ie50685a010.
Shanghai Royal. [Online]. Available: http://www.sa204steel.com/ASME/ASME-SA542-Grade-B-Class-4-alloy-steel-plates-for-pressure-vessels.html. [Accessed: 10-Aug-2020].
Suhan, M.B.K., Shuchi, S.B., Abir, M.R.A.R., Hasan, R., 2019. Innovative multi-stage anaerobic modelling of a 10 mw biogas plant using Aspen HYSYS. In. ICPE 2019, 25.
Zhao, Q.G., Liao, H., Li, S.F., 2000. The effect of pressure, temperature, and particle shape on the pressure drop in fixed bed. Chem. Reaction Eng. Tech. 16 (1), 1–6.